Analysis of a bipolar upward lightning flash based on simultaneous records of currents and 380-km distant electric fields

Amirhossein Mostajabi, Dongshuai Li, Mohammad Azadifar, Farhad Rachidi, Marcos Rubinstein, Gerhard Diendorfer, Wolfgang Schulz, Hannes Pichler, Vladimir Rakov, Davide Pavanello

Analysis of a Bipolar Upward Lightning Flash Based on Simultaneous Records of Currents and 380-km Distant Electric Fields

Amirhossein Mostajabi[1], Dongshuai Li[2], Mohammad Azadifar[3], Farhad Rachidi[1], Marcos Rubinstein[3], Gerhard Diendorfer[4], Wolfgang Schulz[4], Hannes Pichler[4], Vladimir A. Rakov[5,6], Davide Pavanello[7]

1 Electromagnetic Compatibility Laboratory, Swiss Federal Institute of Technology (EPFL), 1015 Lausanne, Switzerland
2 Instituto de Astrofísica de Andalucía (IAA), CSIC, Granada, Spain
3 University of Applied Sciences of Western Switzerland (HES-SO), 1400 Yverdon-les-Bains, Switzerland
4 OVE Service GmbH, Dept. ALDIS, Vienna, Austria
5 Department of Electrical and Computer Engineering, University of Florida, Florida, USA
6 Moscow institute of Electronics and Mathematics, National Research University Higher School of Economics, Moscow
7 University of Applied Sciences of Western Switzerland (HES-SO), 1950 Sion, Switzerland

Corresponding author:
Amirhossein Mostajabi

ELL 036, ELL building, Station 11
1015 Lausanne, Vaud, Switzerland
Tel. +41 21 693 4818
amirhossein.mostajabi@epfl.ch

ABSTRACT

In this paper, we present and discuss simultaneous records of current and wideband electric field waveforms at 380 km distance from the strike point associated with an upward bipolar flash initiated from the Säntis Tower. The flash contains 23 negative strokes and one positive stroke. The intervals between the groundwave and skywave arrival times are used to estimate ionospheric reflection heights for the negative return strokes using the so-called zero-to-zero and peak-to-peak methods. A full-wave, finite-difference time-domain (FDTD) analysis of the electric field propagation including the effect of the ionospheric reflections is also presented. FDTD simulation results are compared with the measured radiated electric field associated with the studied flash to evaluate the reference reflection height of the conductivity profile. It is also found that the ratio of the peak field to the current peak is about two times smaller for the positive pulse compared to negative pulses. This difference in the amplitudes can be attributed to a lower return stroke speed for the positive stroke compared to that for negative strokes, and also to the fact that the enhancement of the electric field due to the presence of the tower and the mountain might be more significant for negative pulses, which are characterized by faster risetimes compared to the positive one.

Keywords—Bipolar lightning flash; simultaneous current and field measurements; ionospheric reflection; field-to-current conversion factor; numerical FDTD simulation

I. INTRODUCTION

In a bipolar flash, the current waveform exhibits a polarity reversal, corresponding to a charge transfer to ground of both negative and positive polarities [1], [2]. Bipolar

flashes are usually initiated by upward leaders from tall structures, but they can also be downward flashes [3].

About 3% of the flashes recorded at the Säntis Tower are bipolar [4]. Fig. 1 shows the monthly distribution of negative, positive and bipolar lightning flashes accumulated over the period ranging from June 2010 to July 2016. It can be seen that positive and bipolar flashes occurred mostly during the warmer seasons (May to October).

Current waveforms associated with bipolar flashes were first reported by McEachron from his studies at the Empire State Building [5]. Further studies on bipolar lightning are based either on lightning current observations (e.g., [4], [6], [7]), or electromagnetic fields, sometimes with high-speed video observations (e.g., [8]–[11]). Only rare observations have been reported that include simultaneous records of currents and fields (e.g., [12]–[14]).

Extremely Low Frequency (ELF) and Very Low Frequency (VLF) electromagnetic field observations, including the radiated electromagnetic fields from distant lightning flashes, have been widely used to examine ionospheric reflection characteristics (e.g., [15]).

Various theoretical and numerical approaches have been proposed to model lightning-ionosphere interactions, which can be divided into four main types [16]:

(i) The first approach, proposed in [17] and [18], is based on solving Maxwell's equations for slabs of a horizontally stratified ionosphere.

(ii) The second approach considers the ionosphere and the earth as boundaries of a waveguide, the so-called Earth-Ionosphere waveguide. This method is based on finding eigenvalues and possible modes of propagation in the assumed waveguide [19], [20].

(iii) In the third method, the ionosphere is modeled as a stack of discrete layers, and the wave propagation is solved using Fresnel equations [21]–[23].

(iv) Finally, the Finite Difference Time Domain (FDTD) method has been used to solve Maxwell's equations in spherical coordinates in order to compute the electromagnetic field interaction with ionospheric layers [24]–[27]. This method is capable of considering a time-varying ionosphere layer and nonlinearities.

In this paper, which is an extended version of [28], we present and discuss simultaneous records of current and wideband electric field waveforms at a 380 km distance from the strike point associated with an upward bipolar flash initiated from the Säntis Tower. The flash was recorded on September 21, 2014 and it contained 23 negative strokes and one positive pulse superimposed on the initial-stage current. The flash belongs to Category I of bipolar flashes according to the classification proposed by Rakov [29]. In this paper, we will treat the positive pulse as a return stroke in the FDTD modelling.

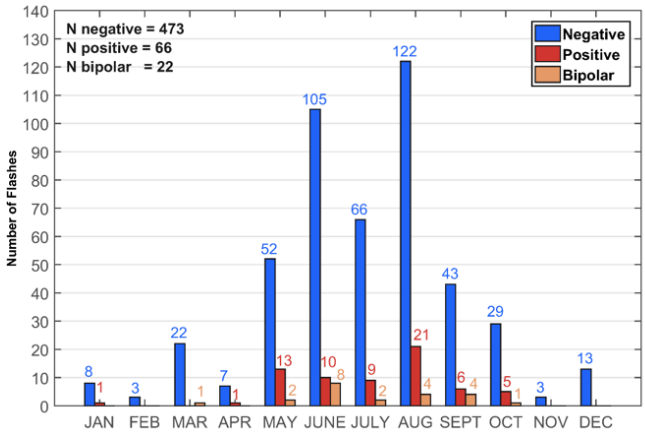

Fig. 1. Monthly distribution of negative, positive and bipolar lightning flashes recorded at Säntis Tower over the period ranging from June 2010 to July 2016.

Further, an FDTD analysis of the field propagation including the effect of the ionospheric reflections is presented and the results are compared with the experimental data for both positive and negative pulses of the studied flash.

The rest of this paper is organized as follows. Section II briefly reviews the instrumentation installed at the Säntis Tower, Switzerland, and the electric field measurement station in Neudorf, Austria. A brief description of the obtained data is presented in Section III. Numerical simulations of the electromagnetic fields obtained using a full-wave FDTD approach and a comparison with the experimental data are presented in Section IV. The analysis and discussion of the results are given in Section V. Finally, conclusions are presented in Section VI.

II. EXPERIMENTAL SETUP AND INSTRUMENTATION

A. Current Measurement System at the Säntis Tower

The 124-m tall Säntis Tower is located on top of the Säntis mountain (2502 m ASL) in Northeastern Switzerland. The tower has been instrumented since May in 2010 using advanced equipment including remote monitoring and control capabilities for accurate measurement of lightning current parameters enabling a high-resolution sampling of lightning currents over long observation windows [30], [3]. The analog outputs of the sensors are relayed to a digitizing system by means of optical fiber links. The system allows over-the-Internet remote maintenance, monitoring, and control.

A PXI platform with a sampling rate of 50 MS/s is used to digitize and record the measured current waveforms. The lightning current is recorded over a 2.4-s time with a pretrigger delay of 960 ms.

In 2013–2014, updates were made to the overall measuring system. More details on the measurement sensors and the instrumentation system can be found in [3], [30]–[33].

B. *Electric Field Measurement System*

Vertical electric fields were measured at a distance of 380 km from the tower (in Neudorf, Northern Austria) by means of a flat-plate antenna. The waveforms were digitized with a sampling rate of 5 MS/s [34]. The antenna was installed on the metal roof of a building with an estimated enhancement factor of about 2.6 [34]. The calibration procedure used by Pichler et al. [34] to determine the field enhancement factor of the antenna was performed using a second identical antenna at ground level, where no field enhancement should be present. Time-correlated measurements of a number of lightning field pulses with both antennas allowed us to determine the field enhancement factor.

The measured field values were corrected to account for this enhancement. The integrator decay time constant was 0.5 ms, corresponding to a lower cutoff frequency of about 300 Hz. The triggering signal was relayed from the Säntis Tower to the field measurement station over the Internet using TCP/IP. The locations of the Säntis Tower and the field measuring station in Neudorf are shown in Fig. 2. More information on the electric field measurement system in Neudorf can be found in [34].

III. OBTAINED DATA

A. *Measurement Data*

We present here an upward bipolar lightning flash recorded on September 21, 2014 at 15:14:09 (local time) along with its associated vertical electric fields in Neudorf, 380 km from the Säntis Tower.

Fig. 3a shows the overall current waveform which contained an Initial Continuous Current (ICC) of negative polarity that lasted for about 320 ms (from 880 to 1200 ms) and included more than 20 superimposed pulses with peak values of about 0.6 to 6.1 kA. The superimposed ICC pulses can be of different types, either M-component-type ICC pulses or mixed mode pulses [34]. A discussion on the characteristics of various types of ICC pulses can be found in [35], [36]. The flash exhibited a polarity reversal during its initial stage, therefore belonging to Category I of bipolar flashes according to the classification proposed by Rakov [29]. It is worth noting that this bipolar flash can also be classified as being of Category III which involves return strokes of opposite polarities. The positive stroke was characterized by a peak current of 39.6 kA and a risetime of 31 μs, which is not far from typical values expected for positive strokes [37]. An expanded view of the initial stage of the current in which the ICC is resolved is shown in the inset of the figure. The vertical electric field associated with this flash is shown in Fig. 3b.

Fig. 2. The location of the Säntis Tower (Switzerland) and the electric field measurement station at Neudorf, Austria. The distance between Neudorf and the Säntis is 380 km.

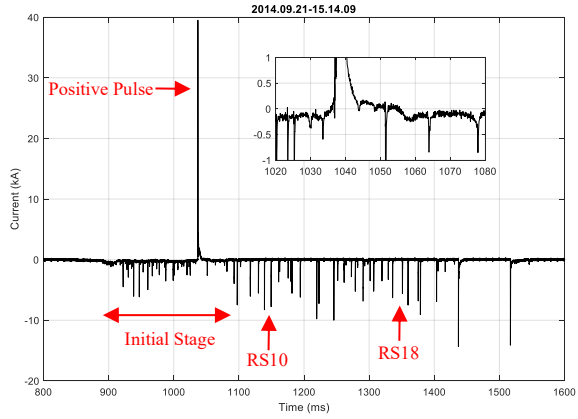

(a)

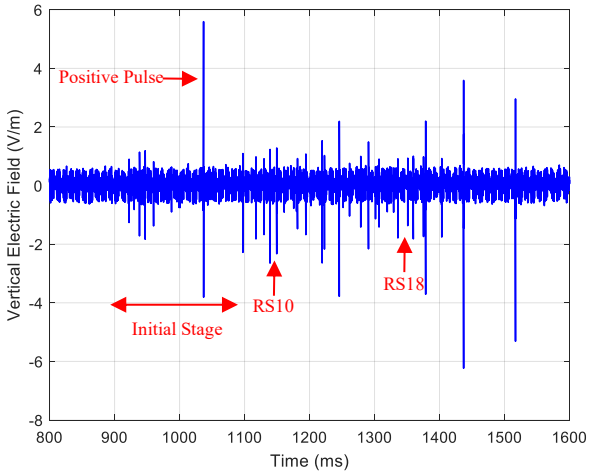

(b)

Fig. 3. Simultaneous current (a) and E-field (b) waveforms associated with a bipolar flash of Category I that occurred on 21 September 2014, at 15:14:09 (local time). The initial stage interval and two of the return strokes (RS10 and RS18) are shown in red. The positive pulse is also shown in red with the label “Positive Pulse”.

Fig. 4 presents the plots of the individual waveforms of the current and the electric field associated with the positive pulse of the bipolar flash (labeled as Positive RS in Fig. 3). Fig. 5 and Fig. 6 present similar plots for two of the negative return strokes of the same flash, labeled as RS10 and RS18 in Fig. 3.

As discussed in [38], 60-kHz ringing can be seen in all the measured E-field waveforms. The origin of this effect is unknown and currently under investigation. It might be due to a malfunction of the integrator at the Neudorf measuring station.

It should be noted that our field measuring system exhibited a high noise level at frequencies of 200, 300, 400 and 500 kHz. In order to reduce the noise, 20-kHz bandwidth notch filters centered at each of the above-mentioned frequencies were applied to all recorded field signals.

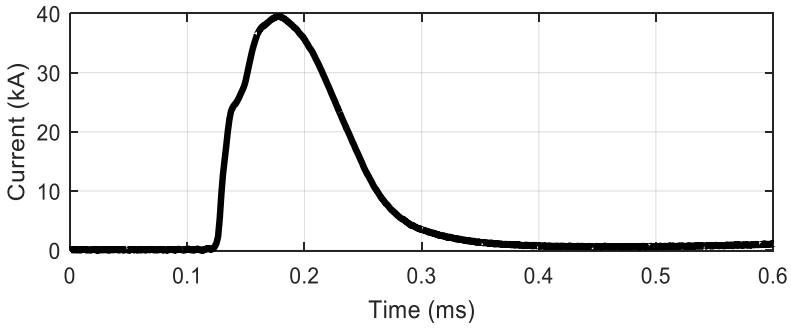

(a)

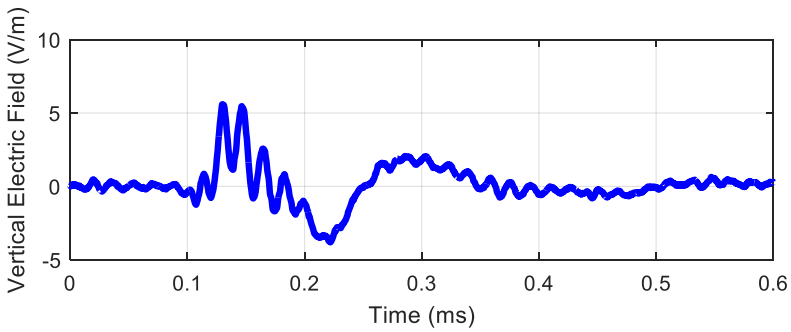

(b)

Fig. 4. Simultaneous current (a) and E-field (b) waveforms associated with the positive pulse of the bipolar flash of 21 September 2014, 15:14:09 (local time).

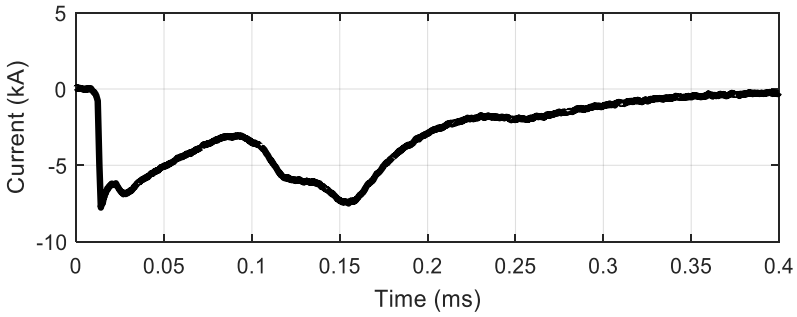

(a)

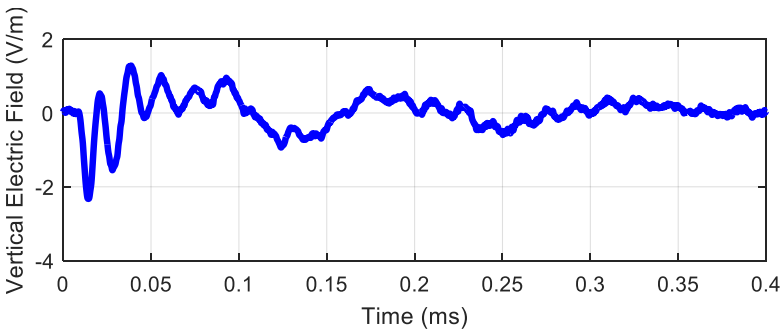

(b)

Fig. 5. Simultaneous current (a) and E-field (b) waveforms associated with a negative return stroke (labeled RS10 in Fig. 3a) of the bipolar flash of 21 September 2014, 15:14:09 (local time).

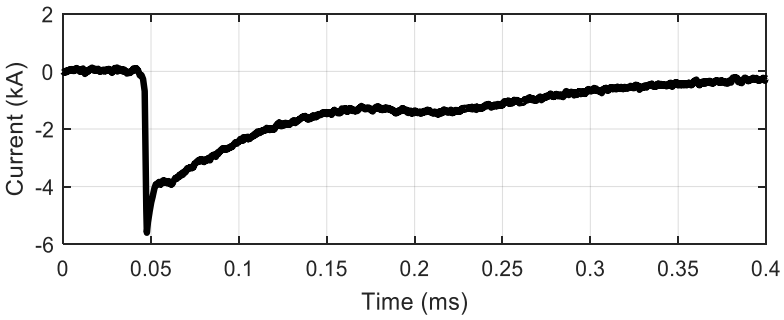

(a)

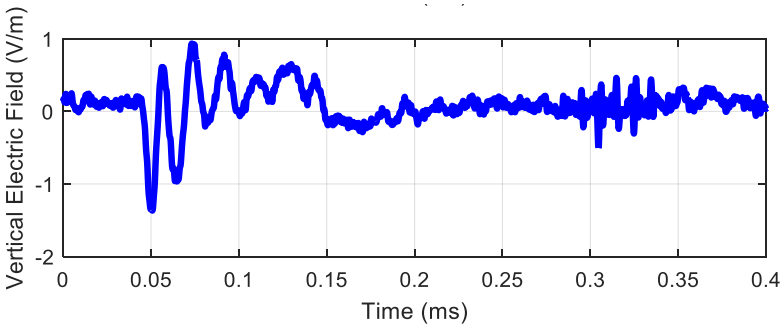

(b)

Fig. 6. Simultaneous current (a) and E-field (b) waveforms associated with a negative return stroke (labeled RS18 in Fig. 3a) of the bipolar flash of 21 September 2014, 15:14:09 (local time).

IV. Analysis and Discussion

In this section, we will use the obtained data to infer the height of ionospheric reflection for both negative and positive pulses. Furthermore, we will analyze the relation between the electric-field peak and current peak for the groundwave and the first skywave associated with detected events. In our analysis, we will consider only pulses for which both current and field waveforms were obtained. These include 5 M-component-type ICC pulses, 1 positive stroke, and 18 negative return strokes. Table I presents a summary of the peak values and risetimes associated with each of the pulses.

Table II presents the median values and ranges of the measured risetimes for negative return strokes and M-component-type ICC pulses.

Table I. Summary of the peak values and risetimes associated with the considered current pulses belonging to the bipolar flash of 21 September 2014, 15:14:09 (local time).

Pulse number	Type	Peak current (kA)	Risetime (μs)
1	ICC pulse (M-component type)	4.5	21.4
2	ICC pulse (M-component type)	2.9	28.0
3	ICC pulse (M-component type)	6.0	21.4
4	ICC pulse (M-component type)	6.1	8.5
5	ICC pulse (M-component type)	5.0	42.2
6	Positive pulse	39.5	31.0
7	Negative return stroke	6.0	2.6
8	Negative return stroke	5.5	1.8
9	Negative return stroke	8.3	1.1
10	Negative return stroke	7.8	1.3
11	Negative return stroke	6.2	1.4
12	Negative return stroke	9.8	1.5
13	Negative return stroke	7.2	0.5
14	Negative return stroke	10.0	0.6
15	Negative return stroke	5.2	0.9
16	Negative return stroke	6.9	1.0
17	Negative return stroke	6.3	0.7
18	Negative return stroke	5.6	1.1
19	Negative return stroke	7.5	1.0
20	Negative return stroke	6.8	0.7
21	Negative return stroke	9.1	0.9
22	Negative return stroke	6.9	0.7
23	Negative return stroke	13.2	0.3
24	Negative return stroke	12.6	1.3

Table II. Median values and ranges of the risetimes associated with the considered current pulses (except for the positive pulse) belonging to the bipolar flash of 21 September 2014, 15:14:09.

Type	Median risetime (μs)	Minimum risetime (μs)	Maximum risetime (μs)
ICC pulses	21.4	8.5	42.2
Negative return strokes	1.0	0.3	2.6

A. Ionospheric Reflections

Three approaches have been used to estimate the effective ionospheric reflection height using measured distant electromagnetic fields from lightning and estimating the arrival time of the first skywave compared to the groundwave [39], [40].

In this paper, we have used the so-called zero-to-zero and the peak-to-peak approaches [40] to infer the height of the reflection. Fig. 7a and Fig. 7b show sequentially the evaluated reflection heights for all the pulses of the flash that exhibited ionospheric reflections, using the zero-to-zero (Fig. 7a) and the peak-to-peak (Fig. 7b)

approaches. It can be seen that according to the zero-to-zero approach, the evaluated reflection height of the negative ICC pulses and return strokes in this flash range from 73 to 81 km, with an arithmetic mean value of 77.5 km. On the other hand, the inferred heights using the peak-to-peak approach are slightly higher and they range from 74 to 87 km, with an arithmetic mean value of 80.5 km.

The evaluated reflection heights of the positive stroke using the zero-to-zero and the peak-to-peak approaches are respectively equal to 94.9 and 95.1 km, significantly higher than the reflection heights for the negative pulses. It is worth noting that the evaluated reflection heights for the positive stroke might be affected by significant errors due to the concurrent effects of slow risetime and the ringing in the field waveforms.

Changes of ionospheric reflection height for first and subsequent return strokes in downward flashes were reported in [40], [41]. The authors of those studies observed that the reflection height tends to increase with increasing return-stroke peak current. Azadifar et al. [38], in their analysis of negative upward flashes initiated from the Säntis Tower, did not observe any significant variation of the reflection height as a function of stroke order within a flash. As discussed in [38], this might be due to the fact that the peak currents in their recorded upward flashes were much smaller than the downward flashes studied by Somu *et al.* [23].

In our dataset (see Fig. 7), the reflection heights inferred for negative ICC pulses before the positive pulse and for negative return strokes after it are very similar. This is to some extent consistent with the analysis of [40], [41], given that the return-stroke current peaks for negative pulses range from 2.9 to 13.2 kA, while the positive pulse peak is about 40 kA. More data and further analyses are needed to understand the

dependence of the reflection height on the source characteristics (return-stroke current peak, frequency content, polarity, channel geometry, etc.).

B. *Current-to-Field Conversion Factor*

Fig. 8 shows the scatterplots of electric-field peak versus current peak for the groundwave and the first skywave associated with all the detected events. Negative return strokes are shown in blue and the measured positive pulse is shown in red in these figures. The best fit linear regression (forced to go through the origin of coordinates) is also presented.

It can be seen that the ratio of the peak field to the current peak is much smaller (a factor of about 2.3 for the groundwave and 1.6 for the first skywave) for the positive pulse compared to negative pulses. Among the reasons that could explain this difference are:

- The return stroke speed for positive strokes is, in general, smaller than that for negative strokes [42]–[44];

- The enhancement of the electric field due to the presence of the tower and the mountain [45]–[49] might be more significant for negative pulses, which are characterized by faster risetimes, than for positive pulses. In the case of the studied flash in this paper, the average risetime of the negative strokes was 6.6 μs, whereas this value was 31 μs for the positive stroke.

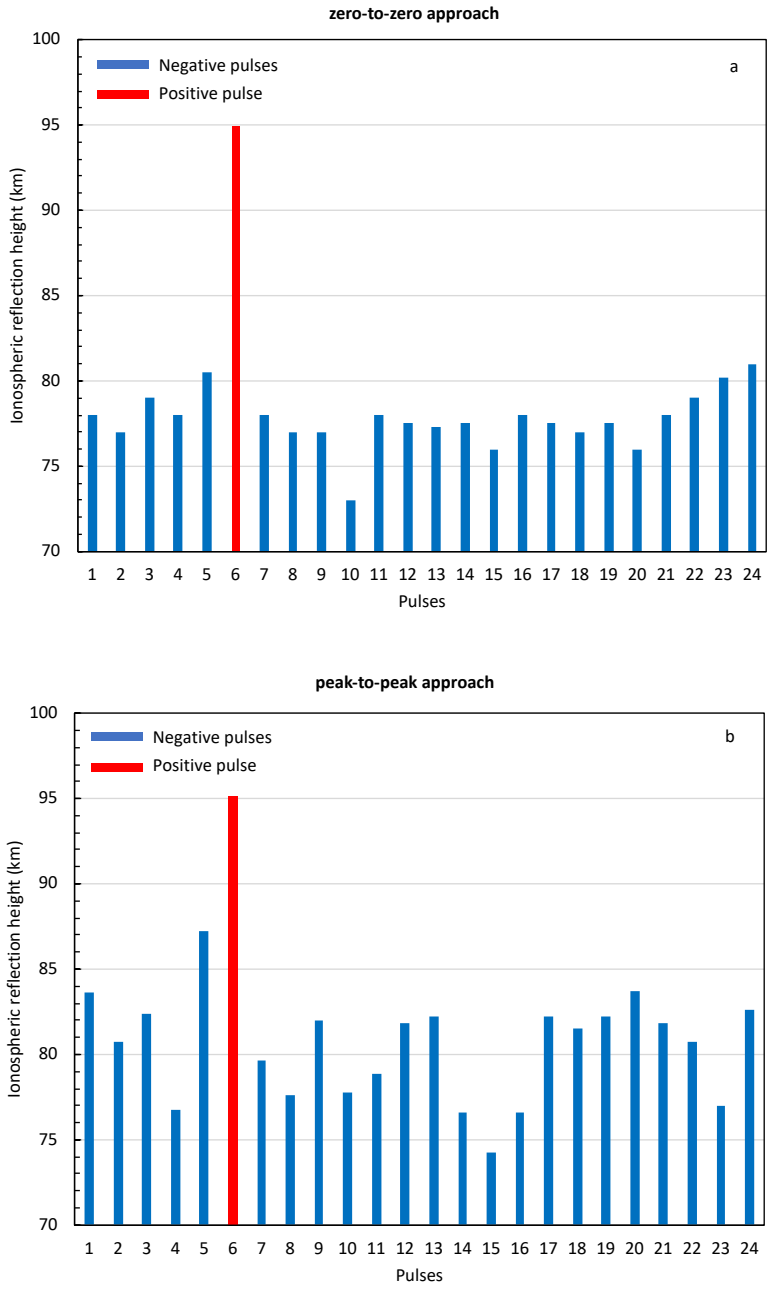

Fig. 7. Sequence of evaluated reflection heights for 23 negative and one positive pulses of the flash of 21 September 2014, 15:14:09 (local time) using a) zero-to-zero approach and b) peak-to-peak approach.

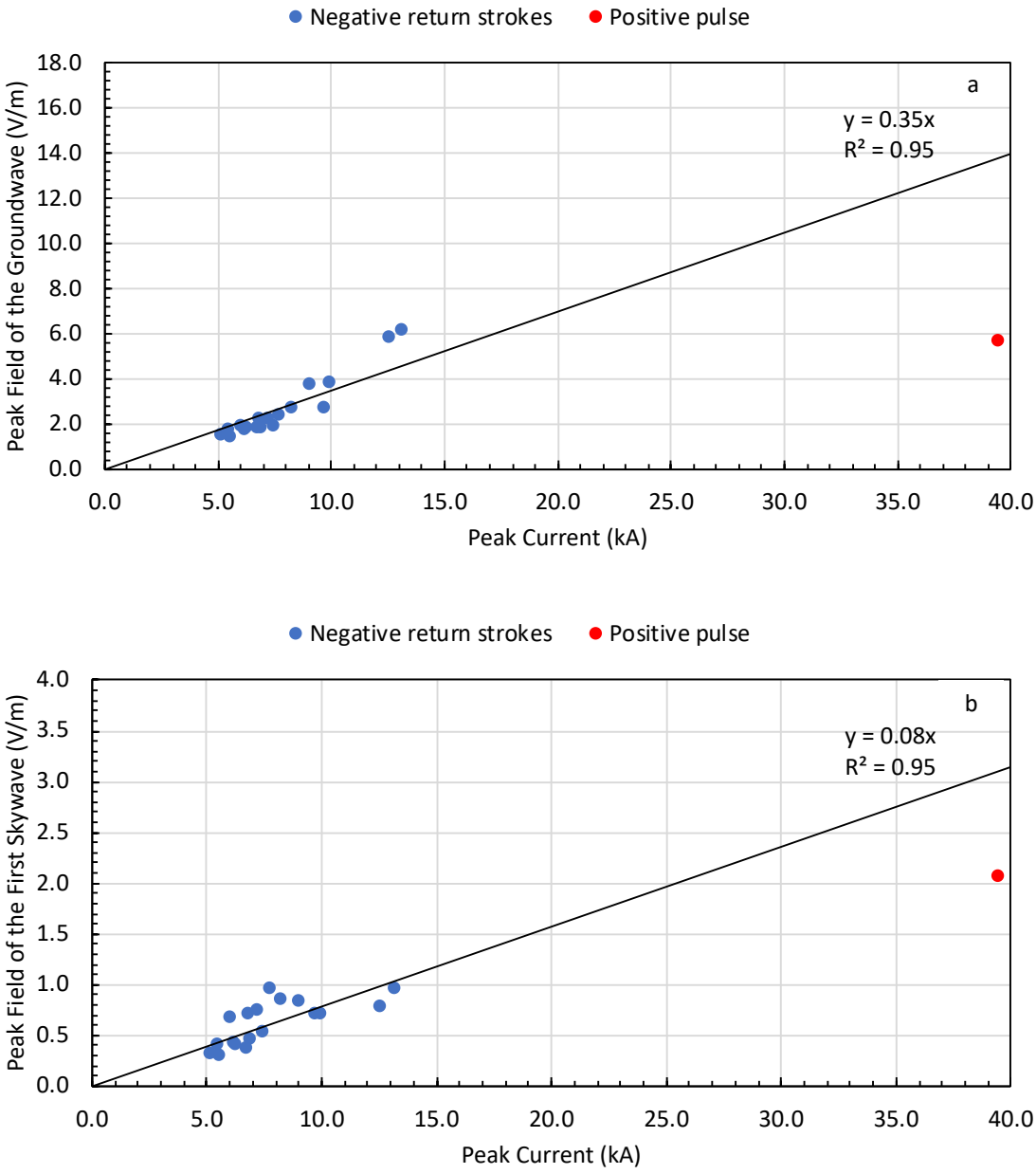

Fig. 8. Electric-field peak of a) the groundwave and b) the first skywave at 380 km versus current peak for all the pulses of the flash of 21 September 2014, 15:14:09 (local time). The positive pulse is shown in red and the 18 negative pulses are shown in blue. The best fit linear regression for negative return strokes is also shown in the figure.

V. FDTD MODELING AND COMPARISON WITH EXPERIMENTAL DATA

A. FDTD Modeling

A full-wave FDTD model was developed and the simulation results were compared with the experimental data for both positive and negative pulses of the studied flash. As shown in Fig. 9, the FDTD calculation domain includes the Earth-Ionosphere Waveguide (EIWG) with a curved ground. The FDTD model uses a two-dimensional spherical coordinate system, as previously done by Bérenger [50]. The lightning channel was set in the symmetry axis of the model and the observation point is at a distance *d* from the lightning source. The entire calculation domain is 500 km × 100 km with a space step of 100 m. Ten layers of the convolutional perfectly matched layer (CPML) absorbing boundary [51] are adopted to avoid reflections from the walls of the computational domain. The ground is assumed to be perfectly conducting. The conductivity of the ionospheric region is given by Wait and Spies [52],

$$\boldsymbol{\sigma(z) = \left(2.5 \times 10^5\right) e^{\beta(z-h)}} \tag{1}$$

where $\boldsymbol{\beta}$ is the typical slope value of the D-region conductivity profile for daytime conditions and $\boldsymbol{h}$ is the reference reflection height (note that h is a parameter and not the reflection height) of the conductivity profile. The height of the lightning channel (H) was assumed to be 8 km and the return stroke speed was assumed to be $\boldsymbol{v = 1.5 \times 10^8}$ m/s for the negative strokes, and two values of speed, $\boldsymbol{v = 1.5 \times 10^8}$ m/s or $\boldsymbol{0.75 \times 10^8}$ m/s were employed for the positive pulse. For both negative and positive strokes, we used the modified transmission line model with exponential current decay with height (MTLE) [53], [54] with current decay constant $\boldsymbol{\lambda = 2\ km}$ [53]. Equation (1) has two adjustable parameters, $\boldsymbol{h}$ and $\boldsymbol{\beta}$. The values of these parameters were selected to obtain

the best match between the measurements and the FDTD simulations based on the method proposed in [55]. Note that the estimated field enhancement factor of about 2.6 due to the effect of the building at the Neudorf station [56] is considered in all the modeling results. In the simulation, the measured currents obtained at the Säntis Tower were used as input, and the electric field waveforms at 380 km were calculated.

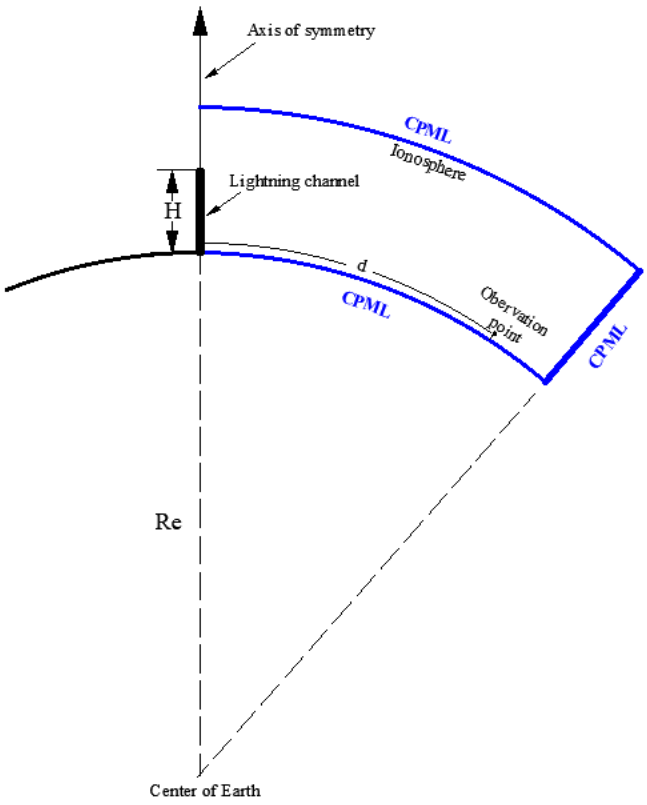

Fig. 9. The geometry of the FDTD model.

Fig. 10, Fig. 11, and Fig. 12 show the comparison results between the FDTD simulation and the experimental data for the positive and negative pulses of the studied bipolar flash. Because of the difficulties associated with the use of the zero-to-zero and peak-to-peak approaches to infer the reflection height, especially when the waveforms are affected by noise, we have determined the reference reflection height in (1) for each

case by trial and error to obtain the best match with the observed experimental waveforms.

It can be seen that the FDTD simulation results are in good agreement with the measured data by assuming a reference height of 77 km for the positive return stroke (Positive RS), and a reference height of 70 km for two negative strokes (RS10 and RS18). Note that these values are smaller than the values inferred in the previous section using the zero-to-zero and the peak-to-peak methods.

The effect of the return-stroke speed for the positive pulse is also shown in Fig. 10, where it can be seen that the return stroke speed can significantly affect the field, especially in its early-time response.

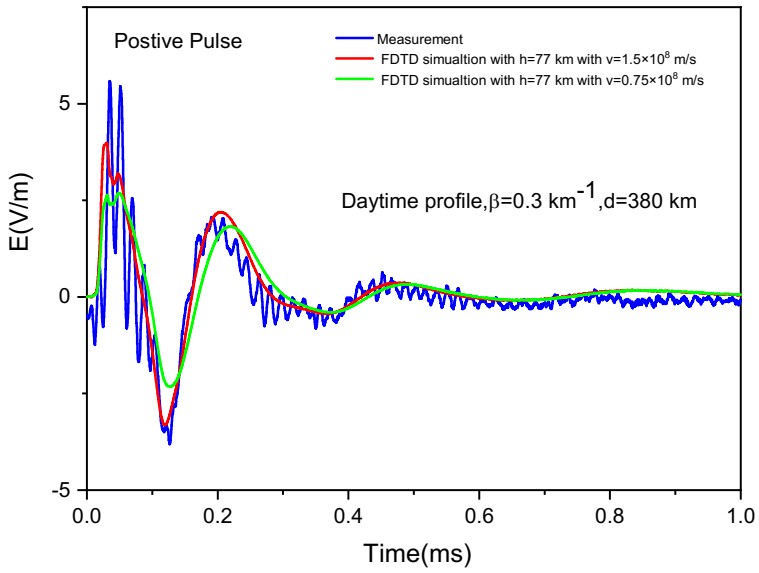

Fig. 10. Comparison between the FDTD simulation and experimental data for the positive pulse (Positive RS in Fig. 3a) of the bipolar flash of 21 September 2014, 15:14:09 (local time) considering the return-stroke speed 1.5×10^8 m/s (red line) and 0.75×10^8 m/s (green line). $\boldsymbol{h = 77}$ km and $\boldsymbol{\beta = 0.3}$ km^{-1} were adjustable parameters that were varied to achieve the best match to the measured waveform.

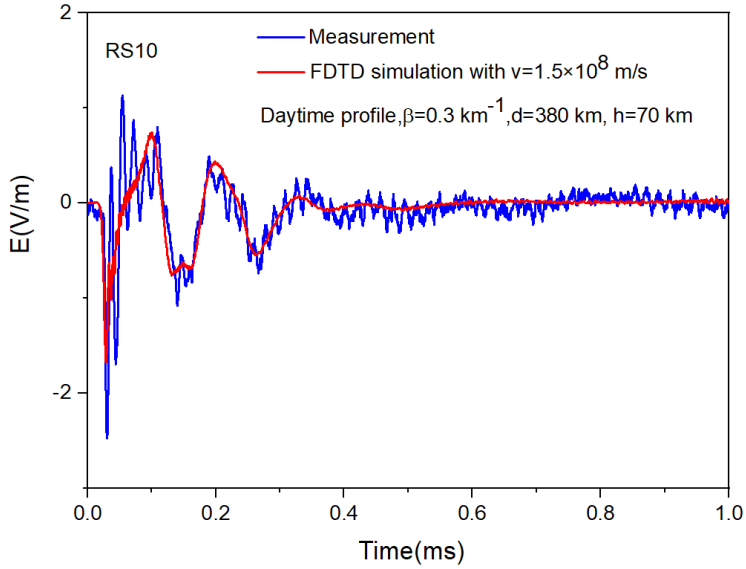

Fig. 11. Comparison between the FDTD simulation and experimental data for the negative return stroke labeled RS10 (in Fig. 3a) of the bipolar flash of 21 September 2014, 15:14:09 (local time).

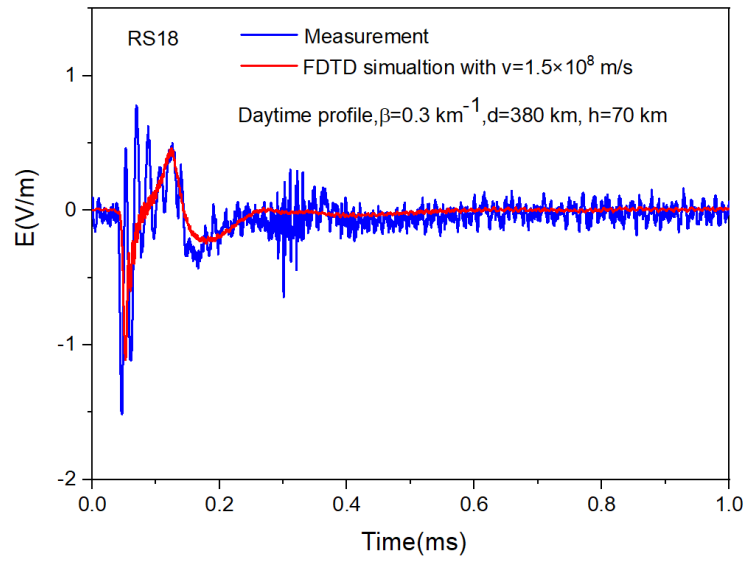

Fig. 12. Comparison between the FDTD simulation and experimental data for the negative return stroke labeled RS18 (in Fig. 3a) of the bipolar flash of 21 September 2014, 15:14:09 (local time).

Note that, in this analysis, we assumed a vertically inhomogeneous, highly collisional and isotropic ionosphere environment as presented by Said [57]. However, during day time, the electron density in the D region of the ionosphere might change with the solar zenith angle and solar flare X-ray fluxes [58], [59].

VI. CONCLUSION

We presented and discussed simultaneous records of current and wideband electric-field waveforms at 380 km distance from the strike point associated with a bipolar upward flash initiated from the Säntis Tower. The recorded flash contained 23 negative and one positive strokes.

It was found that the ratio of the peak field to the current peak is about two times smaller for the positive pulse compared to negative pulses.

Good agreement in the time delay from the groundwave to the first skywave was observed between the measured electric-field waveforms and FDTD simulations using a return-stroke speed of 1.5 x 10^8 m/s both for negative strokes and for the positive pulse.

The reflection heights for negative pulses inferred using the zero-to-zero and the peak-to-peak approaches were found to be in good agreement with the values inferred by the FDTD simulations. On the other hand, for the positive pulse, both the zero-to-zero and the peak-to-peak approaches were found to overestimate the reflection height compared to the FDTD simulations.

ACKNOWLEDGMENT

Financial supports from the Swiss National Science Foundation (Project No. 200021_147058) and the European Union's Horizon 2020 research and innovation program (grant agreement. No 737033-LLR) are acknowledged. All the measured data on lightning current and associated electric field presented in this paper are accessible at the EMC Laboratory of EPFL (farhad.rachidi@epfl.ch).

REFERENCES

[1] M. Azadifar *et al.*, "An update on the charaterictics of positive flashes recorded on the Säntis Tower," *2014 International Conference on Lightning Protection (ICLP)*. pp. 777–781, 2014.

[2] C. Romero, M. Rubinstein, F. Rachidi, M. Paolone, V. A. Rakov, and D. Pavanello, "Some characteristics of positive and bipolar lightning flashes recorded on the Säntis tower in 2010 and 2011," *2012 International Conference on Lightning Protection (ICLP)*. pp. 1–5, 2012.

[3] M. Azadifar, M. Paolone, D. Pavanello, F. Rachidi, C. Romero, and M. Rubinstein, "An Update on the Instrumentation of the Säntis Tower in Switzerland for Lightning Current Measurements and Obtained Results," in *CIGRE Int. Colloquium on Lightning and Power Systems*, 2014.

[4] M. Azadifar, F. Rachidi, M. Rubinstein, V. A. Rakov, M. Paolone, and D. Pavanello, "Bipolar lightning flashes observed at the Säntis Tower: Do we need to modify the traditional classification?," *J. Geophys. Res. Atmos.*, vol. 121, no. 23, p. 14,117-14,126, 2016.

[5] K. B. McEachron, "Lightning to the empire state building," *J. Franklin Inst.*, vol. 227, no. 2, pp. 149–217, 1939.

[6] K. Narita, Y. Goto, H. Komuro, and S. Sawada, "Bipolar lightning in winter at Maki, Japan," *J. Geophys. Res. Atmos.*, vol. 94, no. D11, pp. 13191–13195, Sep. 1989.

[7] W. Schulz and G. Diendorfer, "Bipolar flashes detected with lightning location systems and measured on an instrumented tower," in *Proceedings of the VII International Symposium on Lightning Protection*, 2003, pp. 6–9.

[8] M. Miki, A. Wada, and A. Asakawa, "Observation of upward lightning in winter at the coast of Japan Sea with a high-speed video camera," in *Proc. 27th Int. Conf. Lightning Protection, 1a2*, 2004, pp. 63–67.

[9] M. M. F. Saba, C. Schumann, T. A. Warner, J. H. Helsdon, W. Schulz, and R. E. Orville, "Bipolar cloud-to-ground lightning flash observations," *J. Geophys. Res. Atmos.*, vol. 118, no. 19, p. 11,098-11,106, Oct. 2013.

[10] A. C. V Saraiva *et al.*, "High-speed video and electromagnetic analysis of two natural bipolar cloud-to-ground lightning flashes," *J. Geophys. Res. Atmos.*, vol. 119, no. 10, pp. 6105–6127, May 2014.

[11] H. Zhou, G. Diendorfer, R. Thottappillil, H. Pichler, and M. Mair, "Characteristics of upward bipolar lightning flashes observed at the Gaisberg Tower," *J. Geophys. Res.*, vol. 116, no. D13, p. D13106, Jul. 2011.

[12] F. Heidler, W. Zischank, and J. Wiesinger, "Statistics of lightning current parameters and related nearby magnetic fields measured at the Peissenberg tower," in *Proc. 25th Int. Conf. on Lightning Protection, Rhodes, Greece*, 2000, pp. 78–83.

[13] J. Jerauld, M. A. Uman, V. A. Rakov, K. J. Rambo, and D. M. Jordan, "A triggered lightning flash containing both negative and positive strokes," *Geophys. Res. Lett.*, vol. 31, no. 8, p. n/a-n/a, Apr. 2004.

[14] D. Wang and N. Takagi, “Characteristics of upward bipolar lightning derived from simultaneous recording of electric current and electric field change,” *Proc. URSI E*, vol. 6, p. 2, 2008.

[15] U. S. Inan, S. A. Cummer, and R. A. Marshall, “A survey of ELF and VLF research on lightning-ionosphere interactions and causative discharges,” *J. Geophys. Res. Sp. Phys.*, vol. 115, no. A6, p. n/a-n/a, Jun. 2010.

[16] M. Azadifar, “Characteristics of Upward Lightning Flashes,” Swiss Federal Institute of Technology, 2017.

[17] M. L. V. Pitteway, “The Numerical Calculation of Wave-Fields, Reflexion Coefficients and Polarizations for Long Radio Waves in the Lower Ionosphere. I.,” *Philos. Trans. R. Soc. A Math. Phys. Eng. Sci.*, vol. 257, no. 1079, pp. 219–241, Mar. 1965.

[18] W. R. Piggott, M. L. V. Pitteway, E. V. Thrane, and F. R. S. J. A. Ratcliffe, “The Numerical Calculation of Wave-Fields, Reflexion Coefficients and Polarizations for Long Radio Waves in the Lower Ionosphere. II,” *Philos. Trans. R. Soc. A Math. Phys. Eng. Sci.*, vol. 257, no. 1079, pp. 243–271, Mar. 1965.

[19] R. A. Pappert and J. A. Ferguson, “VLF/LF mode conversion model calculations for air to air transmissions in the earth-ionosphere waveguide,” *Radio Sci.*, vol. 21, no. 4, pp. 551–558, Jul. 1986.

[20] K. G. Budden, *The wave-guide mode theory of wave propagation*. Logos Press, 1961.

[21] I. Nagano, S. Yagitani, K. Miyamura, and S. Makino, “Full-wave analysis of elves created by lightning-generated electromagnetic pulses,” *J. Atmos. Solar-Terrestrial Phys.*, vol. 65, no. 5, pp. 615–625, Mar. 2003.

[22] W. Xiang-Yang, I. Nagano, B. Zong-Ti, and T. Shimbo, “Numerical simulation of the penetration and reflection of a whistler beam incident on the lower ionosphere at very low latitude,” *J. Atmos. Terr. Phys.*, vol. 58, no. 10, pp. 1143–1159, Jul. 1996.

[23] M. Azadifar, D. Li, M. Rubinstein, and F. Rachidi, “A semi-analytical simplified approach to compute lightning radiated electric fields at long distances taking into account ionospheric reflection,” in *2017 XXXIInd General Assembly and Scientific Symposium of the International Union of Radio Science (URSI GASS)*, 2017, pp. 1–4.

[24] Tran Huu Thang, V. A. Rakov, Y. Baba, and V. B. Somu, “2D FDTD simulation of LEMP propagation considering the presence of conducting atmosphere,” in *2016 Asia-Pacific International Symposium on Electromagnetic Compatibility (APEMC)*, 2016, pp. 19–21.

[25] W. Hu and S. A. Cummer, “An FDTD Model for Low and High Altitude Lightning-Generated EM Fields,” *IEEE Trans. Antennas Propag.*, vol. 54, no. 5, pp. 1513–1522, May 2006.

[26] M. Cho and M. J. Rycroft, “Computer simulation of the electric field structure and optical emission from cloud-top to the ionosphere,” *J. Atmos. Solar-Terrestrial Phys.*, vol. 60, no. 7–9, pp. 871–888, May 1998.

[27] R. A. Marshall, “An improved model of the lightning electromagnetic field interaction with the D-region ionosphere,” *J. Geophys. Res. Sp. Phys.*, vol. 117, no. A3, p. n/a-n/a, Mar. 2012.

[28] A. Mostajabi *et al.*, “Simultaneous Records of Current and 380-km Distant Electric Field of a Bipolar Lightning Flash,” in *2017 International Symposium on Lightning Protection (XIV SIPDA)*, 2017.

[29] V. A. Rakov, “A Review of Positive and Bipolar Lightning Discharges,” *Bull. Am. Meteorol. Soc.*, vol. 84, no. 6, pp. 767–776, Jun. 2003.

[30] C. Romero *et al.*, “A system for the measurements of lightning currents at the Säntis Tower,” *Electr. Power Syst. Res.*, vol. 82, no. 1, pp. 34–43, 2012.

[31] C. Romero, F. Rachidi, M. Paolone, and S. Member, “Statistical Distributions of Lightning Currents Associated With Upward Negative Flashes Based on the Data Collected at the Säntis (EMC) Tower in 2010 and 2011,” *IEEE Trans. Power Deliv.*, vol. 28, no. 3, pp. 1804–1812, 2013.

[32] C. Romero, A. Mediano, A. Rubinstein, F. Rachidi, A. Rubinstein, and M. Paolone, “Measurement

of Lightning Currents Using a Combination of Rogowski Coils and B-Dot Sensors," *J. Light. Res.*, vol. 4, pp. 71–77, 2012.

[33] C. Romero, F. Rachidi, R. M., P. M., R. V. A., and D. Pavanello, "Positive Lightning Flashes Recorded on the Säntis Tower in 2010 and 2011," *J. Geophys. Res.*, p. 12'879-12'892, 2013.

[34] H. Zhou, V. A. Rakov, G. Diendorfer, R. Thottappillil, H. Pichler, and M. Mair, "A study of different modes of charge transfer to ground in upward lightning," *J. Atmos. Solar-Terrestrial Phys.*, vol. 125–126, pp. 38–49, Apr. 2015.

[35] M. Azadifar *et al.*, "Fast initial continuous current pulses versus return stroke pulses in tower-initiated lightning," *J. Geophys. Res. Atmos.*, vol. 121, no. 11, pp. 6425–6434, Jun. 2016.

[36] L. He *et al.*, "An Analysis of Current and Electric Field Pulses Associated With Upward Negative Lightning Flashes Initiated from the Säntis Tower," *J. Geophys. Res. Atmos.*, vol. 123, no. 8, pp. 4045–4059, Apr. 2018.

[37] CIGRE Working Group C4.407 (V.A. Rakov, A. Borghetti, C. Bouquegneau, W.A. Chisholm, V. Cooray, K. Cummins, G. Diendorfer, F. Heidler, A. Hussein, M. Ishii, C.A. Nucci, A. Piantini, O. Pinto Jr., X. Qie, F. Rachidi, M.M.F. Saba, T. Shindo, W. Schulz, R. Thottappillil, S. Visacro, W. Zischank), "Lightning Parameters for Engineering Applications", Technical Brochure 549, CIGRE, 2014.

[38] M. Azadifar *et al.*, "Analysis of lightning-ionosphere interaction using simultaneous records of source current and 380 km distant electric field," *J. Atmos. Solar-Terrestrial Phys.*, vol. 159, pp. 48–56, Jun. 2017.

[39] T. B. McDonald, M. A. Uman, J. A. Tiller, and W. H. Beasley, "Lightning location and lower-ionospheric height determination from two-station magnetic field measurements," *J. Geophys. Res. Ocean.*, vol. 84, no. C4, pp. 1727–1734, Apr. 1979.

[40] M. A. Haddad, V. A. Rakov, and S. A. Cummer, "New measurements of lightning electric fields in Florida: Waveform characteristics, interaction with the ionosphere, and peak current estimates," *J. Geophys. Res. Atmos.*, vol. 117, no. 10, 2012.

[41] V. B. Somu, V. A. Rakov, M. A. Haddad, and S. A. Cummer, "A study of changes in apparent ionospheric reflection height within individual lightning flashes," *J. Atmos. Solar-Terrestrial Phys.*, vol. 136, pp. 66–79, 2015.

[42] D. Wang, N. Takagi, T. Watanabe, V. A. Rakov, and M. A. Uman, "Observed leader and return-stroke propagation characteristics in the bottom 400 m of a rocket-triggered lightning channel," *J. Geophys. Res. Atmos.*, vol. 104, no. D12, pp. 14369–14376, Jun. 1999.

[43] V. A. Rakov, "Lightning return stroke speed," *J. Light. Res*, vol. 1, pp. 80–89, 2007.

[44] V. P. Idone, R. E. Orville, D. M. Mach, and W. D. Rust, "The propagation speed of a positive lightning return stroke," *Geophys. Res. Lett.*, vol. 14, no. 11, pp. 1150–1153, 1987.

[45] M. Azadifar *et al.*, "Evaluation of the performance characteristics of the European Lightning Detection Network EUCLID in the Alps region for upward negative flashes using direct measurements at the instrumented Säntis Tower," *J. Geophys. Res. Atmos.*, pp. 595–606, 2015.

[46] Y. Baba and V. A. Rakov, "Lightning electromagnetic environment in the presence of a tall grounded strike object," *J. Geophys. Res. Atmos.*, vol. 110, no. D9, p. n/a-n/a, 2005.

[47] Y. Baba and V. A. Rakov, "Lightning strikes to tall objects: Currents inferred from far electromagnetic fields versus directly measured currents," *Geophys. Res. Lett.*, vol. 34, no. 19, p. n/a-n/a, 2007.

[48] J. L. Bermudez *et al.*, "Far-field-current relationship based on the TL model for lightning return strokes to elevated strike objects," *IEEE Transactions on Electromagnetic Compatibility*, vol. 47, no. 1. pp. 146–159, 2005.

[49] D. Li *et al.*, "On Lightning Electromagnetic Field Propagation Along an Irregular Terrain," *IEEE Transactions on Electromagnetic Compatibility*, vol. 58, no. 1. pp. 161–171, 2016.

[50] J.-P. Bérenger, “FDTD computation of vlf-lf propagation in the Earth-ionosphere waveguide,” *Ann. Des Télécommunications*, vol. 57, no. 11–12, pp. 1059–1090, 2002.

[51] J. A. Roden and S. D. Gedney, “Convolution PML (CPML): An efficient FDTD implementation of the CFS-PML for arbitrary media,” *Microw. Opt. Technol. Lett.*, vol. 27, no. 5, pp. 334–339, Dec. 2000.

[52] J. Wait and K. Spies, “Characteristics of the Earth-ionosphere waveguide for VLF radio waves,” *US Dept. Commer. Natl. Bur. Stand. sale by Supt. Doc., US Govt. Print. Off*, 1964.

[53] C. A. Nucci and F. Rachidi, “Experimental validation of a modification to the Transmission Line model for LEMP calculation,” in *8th Symposium and Technical Exhibition on Electromagnetic Compatibility*, 1989.

[54] C. A. Nucci, C. Mazetti, F. Rachidi, and M. Ianoz, “On lightning return stroke models for LEMP calculations,” *Proc. 19th Int. Conf. Light. Prot. Graz, Austria, 1988*, 1988.

[55] X.-M. Shao, E. H. Lay, and A. R. Jacobson, “Reduction of electron density in the night-time lower ionosphere in response to a thunderstorm,” Nat. Geosci., vol. 6, no. 1, pp. 29–33, Jan. 2013.

[56] H. Pichler, G. Diendorfer, and M. Mair, “Some Parameters of Correlated Current and Radiated Field Pulses from Lightning to the Gaisberg Tower,” IEEJ Trans. Electr. Electron. Eng., vol. 5, no. 1, pp. 8–13, Jan. 2010.

[57] R. K. Said, “Accurate and Efficient Long-range Lightning Geo-location Using a VLF Radio Atmospheric Waveform Bank,” Stanford University, 2010.

[58] F. Han, S. A. Cummer, J. Li, and G. Lu, “Daytime ionospheric D region sharpness derived from VLF radio atmospherics,” J. Geophys. Res. Sp. Phys., vol. 116, no. A5, May 2011.

[59] F. Han and S. A. Cummer, “Midlatitude daytime D region ionosphere variations measured from radio atmospherics,” J. Geophys. Res. Sp. Phys., vol. 115, no. A10, p. n/a-n/a, Oct. 2010.